Study of Active Line Flow Constraints in DC Optimal Power Flow Problems

Zhi Jin Zhang, Priya Thekkumparambath Mana, Decheng Yan, Yichen Sun, Daniel K. Molzahn

Abstract—Efficiently and reliably operating electric power grids requires the frequent solution of optimization problems such as the DC Optimal Power Flow (DC OPF) problem. Solution of DC OPF problems can be challenging due to the large number of operational constraints imposed in these problems, especially limits on the line flows. Improving solver times can be facilitated by a better understanding of the active line flow constraints in DC OPF problems (i.e., the inequality constraints limiting line flows that are satisfied with equality at the solution). Considering a variety of test cases and a range of loading scenarios, this paper empirically characterizes the sets of active line flow constraints in DC OPF problems. Among other analyses, the paper compares the sets of redundant line flow constraints (i.e., constraints guaranteed to be inactive) that are identified by previously proposed constraint screening methods to the line flow constraints that are actually observed to be active over a range of scenarios. The results indicate that a large fraction of the line flow constraints which are not identified as being redundant by these screening methods are nevertheless inactive in the DC OPF solutions. This observation suggests the potential for improvements to the constraint screening methods. Laying the groundwork for achieving these improvements, this paper also identifies which line characteristics tend to be associated with active flow constraints and studies the relationships among sets of simultaneously active line flow constraints.

Index Terms—DC Optimal Power Flow, constraint screening.

I. INTRODUCTION

Operating electric power grids requires continuous adaptations to accommodate changes resulting from, e.g., seasonal variations, disturbances, and imbalances associated with varying electricity consumption and fluctuating renewable energy generation. The DC Optimal Power Flow (DC OPF) problem is one of the most important optimization problems that is solved in order to manage system operations.

The DC OPF problem uses the DC power flow approximation to reduce the complexity of AC power systems. The DC power flow approximates the voltage magnitude at each bus as 1 per unit (p.u.) and the phase angle differences between any two adjacent buses are assumed to be small. The objective of the DC OPF problem is to minimize the generation cost while satisfying constraints that restrict the solutions to the physical operating limits of the power grid. Typically, these constraints can be classified into three categories:

1) Balancing constraint: The net power injected at each bus equals the total power flowing into the adjacent lines.
2) Generation constraint: The power supplied by each generator is within its maximum and minimum capabilities.

3) Transmission constraint: The power flowing through each line is within a prescribed flow limit.

The computational complexity resulting from the large number of transmission line constraints challenges DC OPF solution algorithms, particularly when recurring computations are required to operate a time-variant network with changing loads and renewable generation, when solving planning problems that consider many possible scenarios [1], and when solving more complex generalizations of the DC OPF problems, such as DC unit commitment problems [2].

To address this challenge, a number of previously proposed "constraint screening" methods remove redundant constraints in order to speed up the computation of power system optimization algorithms [3]–[7]. These methods rely on the observation that only a small fraction of the line flow constraints are active at solutions to typical DC OPF problems, despite large variations in the load demands and generation costs [8]. Exploiting this observation, the transmission constraints that are statistically unlikely or analytically proven to be inactive can be neglected when solving the optimization problem. This approach saves computation time without introducing inaccuracies in the resulting solutions.

To identify redundant transmission constraints, many constraint screening methods [3]–[7] solve a set of optimization problems that maximize and minimize the power flowing in each line while satisfying all of the DC OPF constraints. If the most extreme achievable power flow on a line is within the specified line flow limit, the corresponding line flow constraint is guaranteed to be redundant (i.e., implied by the other constraints in the DC OPF problem) and can therefore be neglected. Related analytical screening methods can also quickly identify redundant flow constraints on parallel lines without solving optimization problems [6], [9]. Other recent research applies learning techniques to identify the sets of active constraints in DC OPF problems [8].

A range of operational conditions can be considered in these constraint screening methods by modeling the net load demands as variables contained within a specified load variability set [6]. For typical DC OPF problems, these constraint screening methods are capable of identifying a large fraction of the line flow constraints as being redundant, even when considering a wide range of variation in the net loads [6]. Thus, these methods facilitate off-line analyses for a range of operational conditions, the results of which are useful for speeding up the solution of on-line DC OPF computations.

The computational advantages resulting from the removal of redundant line constraints has already been demonstrated in prior literature, e.g., a 20.7% to 95.6% speed improvement

The authors are affiliated with the School of Electrical and Computer Engineering, Georgia Institute of Technology, Atlanta, GA 30332, USA. Email: {justin.zhang, priya.tm, decheng.yan, yichen.casillas.sun, molzahn}@gatech.edu.

is observed in [6]. Hence, rather than focus on these speed improvements themselves, we aim to study the effectiveness of the constraint screening algorithms. Specifically, this paper compares and characterizes the sets of line flow constraints that are *potentially* active (i.e., the constraints not identified as redundant by a constraint screening method) and the sets of line flow constraints that are *actually observed* to be active as obtained from solving the DC OPF problem, for different ranges of load variation.

First, an optimization-based constraint screening method is implemented to identify the potentially active line flow constraints for a range of load variations. A set of DC OPF problems are then solved, sampling from the same range of load variations while the generation cost is also varied. The actually active line flow constraints are recorded from the DC OPF solutions for each loading scenario. Based on our results, we observe that a gap exists between the number of potentially active line flow constraints identified by a screening method and the number of observed active line flow constraints. This gap is bigger for larger test cases. We also identify some physical characteristics (based on the lines' reactances and flow limits) that indicate which line flow constraints are likely to be inactive. Furthermore, we study the relationships among the sets of lines that are simultaneously active in various DC OPF solutions.

This paper is organized as follows: Section II reviews the DC optimal power flow problem and introduces the optimization-based constraint screening method we employ in our analyses. Section III describes our methodology for DC OPF calculation for a large number of load demands and cost variations. Section IV discusses simulation results and observations from the constraint screening method and from the DC OPF solutions. Section V concludes the paper.

II. BACKGROUND REVIEW

This section briefly describes the fundamental concepts used in this work. The standard DC OPF formulation is described first, followed by a review of constraint screening methods [3]–[7].

The DC power flow is based on the following assumptions:

$$\sin(\theta_i - \theta_j) \approx \theta_i - \theta_j \tag{1a}$$

$$|g_{ij}| \ll |b_{ij}| \tag{1b}$$

$$v_i \approx 1 \tag{1c}$$

where θ_i and θ_j are the voltage angles at the connected buses i and j, respectively; g_{ij} and b_{ij} denote the conductance and susceptance, respectively, between buses i and j; and v_i is the voltage magnitude at bus i. Extensions to more detailed DC power flow formulations [10] are straightforward.

A. DC Optimal Power Flow

We denote the set of buses by $\mathcal{V}$ and the set of transmission lines by $\mathcal{L}$. The set of generator buses is $\mathcal{G} \subseteq \mathcal{V}$. The vector d encodes the load demand at each bus. The limits on generator power outputs and line flows are p^{max}, p^{min}, and f^{max}, respectively. By adjusting the decision variables p and θ, where p denotes generator outputs, the objective

of the optimal power flow problem is to minimize the total generation cost while satisfying the requirement of generation and load balance, abiding by all constraints imposed by power limits on generators and flow limits on transmission lines:

$$\min_{p,\theta} \quad \sum_{i \in \mathcal{G}} c_{0,i} + c_{1,i}\, p_i + c_{2,i}\, p_i^2 \tag{2a}$$

$$\text{subject to} \quad p_i - d_i = \sum_{j:(i,j)\in\mathcal{L}} b_{ij}(\theta_i - \theta_j), \quad \forall\, i \in \mathcal{V} \tag{2b}$$

$$-f_{ij}^{max} \le b_{ij}(\theta_i - \theta_j) \le f_{ij}^{max}, \,\forall\, ij \in \mathcal{L} \tag{2c}$$

$$p_i^{min} \le p_i \le p_i^{max}, \qquad\qquad \forall\ i \in \mathcal{G} \tag{2d}$$

The parameters $c_{0,i}$, $c_{1,i}$, and $c_{2,i}$ are specified constant, linear, and quadratic coefficients for the cost of the power produced by generator $i \in \mathcal{G}$.

B. An Optimization-Based Constraint Screening Method

We next review the constraint screening method that is employed in the remainder of this paper, which is closely related to the approach in [6]. To identify the line flow constraints that can potentially be active over a range of varying load, we find the maximum and minimum power flows that can potentially occur on each transmission line for any loading scenario within a specified load variation set $\mathcal{D}$. Thus, in addition to p and θ, we consider d, which varies within $\mathcal{D}$, as another decision variable in order to identify the maximum and minimum power flows on every line, denoted as f_{mn}^*. For each line $(m,n) \in \mathcal{L}$, the constraint screening method solves the following optimization problems to compute f_{mn}^*:

$$\max_{p,\theta,d} / \min_{p,\theta,d} \ f_{mn} \tag{3a}$$

$$\text{subject to} \quad f_{mn} = b_{mn}(\theta_m - \theta_n), \tag{3b}$$

$$p_i - d_i = \sum_{j:(i,j)\in\mathcal{L}} b_{ij}(\theta_i - \theta_j), \quad \forall\, i \in \mathcal{V} \tag{3c}$$

$$-f_{ij}^{max} \le b_{ij}(\theta_i - \theta_j) \le f_{ij}^{max}, \,\forall\, ij \in \mathcal{L} \tag{3d}$$

$$p_i^{min} \le p_i \le p_i^{max}, \qquad\qquad \forall\ i \in \mathcal{G} \tag{3e}$$

$$d \in \mathcal{D} \tag{3f}$$

The following condition is sufficient to certify that the flow limit on the line $(m,n) \in \mathcal{L}$ is inactive for all loading conditions within the specified variability set $\mathcal{D}$:

$$f_{mn}^* < f_{mn}^{max} \qquad \text{for the maximization problem and}$$
$$f_{mn}^* > -f_{mn}^{max} \quad \text{for the minimization problem}$$

Hence, the line flow limit (2c) is redundant for this line and can be neglected without affecting the solution to the DC OPF problem. Repeating this process for every line $(m,n) \in \mathcal{L}$ generates a set of redundant/inactive lines, which we denote as $\mathcal{R}$. Using the results of this optimization-based screening method, we can solve the original DC OPF problem with a reduced set of line constraints, i.e., $\mathcal{L} \backslash \mathcal{R}$ rather than $\mathcal{L}$ in (2c).

III. DC OPF SAMPLING METHODOLOGY

The objective of the above-mentioned constraint screening method (3) is to maximize and minimize line flows without

violating any physical constraints. Since the cost function (2a) is not considered in the screening method, the results of this method only provide the *potentially* active line flow limits, namely, the flow limits not identified as redundant by the constraint screening method which can thus possibly be reached. However, practically, some potentially active lines may never reach their limits in the solutions to DC OPF problems due to the flow patterns resulting from particular generator costs. Excluding the line flow limits which may potentially be active (according to the screening method) but are not observed to be active in any DC OPF solutions, the remaining lines are called actually/observed active lines, which are a subset of potentially active lines. One objective of this paper is to explore the gap between the sets of potentially active and observed active line flow constraints.

To accomplish this, we will compare results from the screening method and a DC OPF sampling method. Concretely, the latter differs from the former in two aspects:

1) Generation costs are considered and the objective of the optimization problem is to minimize generation cost without violating any physical constraints.
2) The load demand is given as a discrete value, whereas the screening method considers a load variation range.

Hence, to quantitatively analyze the sets of non-redundant line constraints for each load range, we need to solve multiple DC OPF problems with load demands sampled from the given load variation range and compare the associated active line flow constraints with the screening method results.

This sampling approach selects 1,000 random discrete load scenarios of all load demands within the given load variation range for each test case and each load variation range, e.g., $\pm 25\%$ of the nominal load demands. Furthermore, we consider ten randomly selected, non-negative linear generator cost functions (i.e., $c_{2,i} = 0$, $c_{1,i} \geq 0$ for all $i \in \mathcal{G}$) for each load variation range. Thus, in total, we solve DC OPF problems for $10^3 \cdot 10 = 10^4$ load–cost combinations for each test case. The active line flow limits are recorded for each combination. The reason to choose loads and cost coefficients randomly is to (i) disregard their ratios that may bias the results and (ii) obtain a large collection of observed active line flow constraints.

IV. RESULTS AND ANALYSIS

The constraint screening method in [6] is implemented in MATLAB using CVX [11] and the DC OPF analysis is implemented in MATPOWER [12]. We selected test cases from PGLib v.19.05 [13] as summarized in Table I.

For the sake of brevity, only a subset of the test cases will be discussed in detail. The other test cases give qualitatively similar results. Note that in this work, the following load variation ranges are considered for both the screening method and the DC OPF solutions:

$$(1 - \delta) \times d_i^{nom} \leq d_i \leq (1 + \delta) \times d_i^{nom}, \qquad (4)$$

where d_i^{nom} is the nominal load value at each bus i and δ is the variation parameter with values of $\delta = \{0, 0.25, 0.5, 0.75, 1\}$ that correspond to load variations of 0%, $\pm 25\%$, $\pm 50\%$, $\pm 75\%$, and $\pm 100\%$, respectively.

TABLE I: Summary of Test Cases.

Case Name	Number of Lines
case3_lmbd	3
case5_pjm	6
case24_ieee_rts	38
case30_as	41
case30_fsr	41
case30_ieee	41
case39_epri	46
case57_ieee	80
case73_ieee_rts	120
case89_pegase	210
case118_ieee	186
case162_ieee_dtc	284
case179_goc	263
case200_tamu	245
case240_pserc	448
case300_ieee	411
case2383wp_k	2896

A. Visual Representation of Redundant and Active Constraints

Fig. 1 and Fig. 2 represent the network diagrams for the IEEE 24-bus reliability test system (RTS) and the IEEE 118-bus system, respectively. The lines identified as potentially active by the constraint screening method are shown in yellow. The lines that are both potentially active and actually observed to be active in at least one DC OPF solution are shown in red. All other lines, shown in green, are identified as redundant by the constraint screening method. Note that, as expected, all of the actually active lines were also identified as being potentially active by the screening method.

Although it is difficult to predict which of the potentially active lines will be observed to be actually be active after repeated DC OPF simulations, we make several observations. In the IEEE 24-bus system shown in Fig. 1, bus 7 is a generator bus, whereas other buses in the vicinity (3, 4, 5, 6, 8, 9, and 10) are all load buses. Since there is a single line connecting bus 7 to bus 8, it is not surprising that this line has an active constraint in the DC OPF solutions. The next set of lines from bus 8, lines 8-9 and 8-10, also have active flow constraints. Because buses 1, 2, and 7 are the only generator buses in this part of the system, the constraint screening method identifies that most of the lines surrounding them may be active constraints. However, the DC OPF analysis reveals that not all these lines are actually active constraints.

In the IEEE 118-bus system shown in Fig. 2, the lines connecting clusters of buses are both identified as potentially active and observed to be actually active constraints. Examples include lines 38-65, 49-66, 100-103, etc. Most buses that have four or more connecting lines also have at least one or more active line flow limits (e.g., buses 49, 69, 77, 80, 100, etc.).

While such analytical observations using the network layouts are possible for small cases, this approach is challenging for larger systems. The following subsections discuss other analyses and patterns observable in the potentially active, actually active, and redundant line constraints for larger cases.

B. Number of Active Constraints for Varying Ranges of Load

In this analysis, both the constraint screening method and the DC OPF are run for the five different load variation ranges
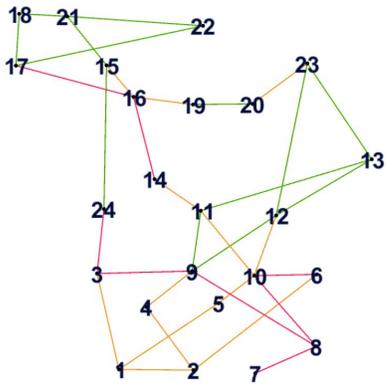
Fig. 1: Case24_ieee_rts: green – redundant, yellow – potentially active, and red – potentially and actually active line flow constraints.
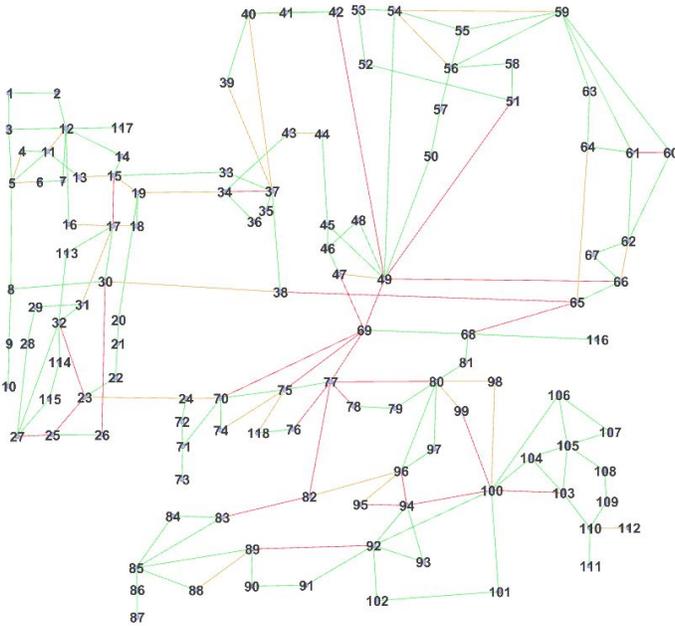

Fig. 2: Case118_ieee: green – redundant, yellow – potentially active, and red – potentially and actually active line flow constraints.

mentioned earlier. For each load range, the number of potentially active constraints identified by the screening method and actually active constraints observed in the 10,000 random samples of DC OPF problems is demonstrated in Fig. 3 for case39_epri, case57_ieee, case118_ieee, and case2383wp_k.

Firstly, all the plots in Fig. 3 show that both the number of potentially active line flow limits (obtained from the constraint screening method) and the actually active line flow limits (obtained from repeated DC OPF solves) increase with larger ranges of load variation. This is expected because when the load constraint is relaxed, the loads can vary over a large range and have substantial differences from normal operating conditions. This enlarges the feasible space of (3) and may lead to higher line flows in some lines, resulting in these line flow limits becoming active.
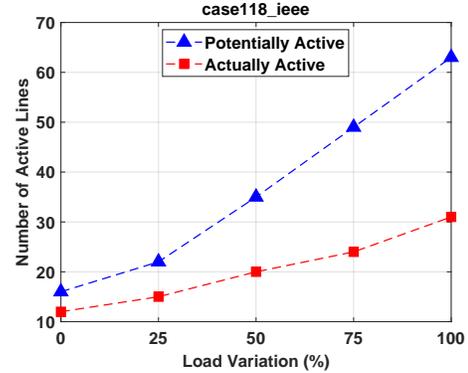
We also observe that the gap between the number of potentially and actually active line flow limits (i.e., the gap between the red and blue lines) becomes larger as load variation range increases in all test cases with more than 100
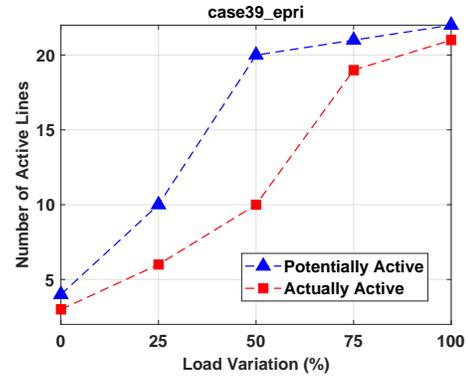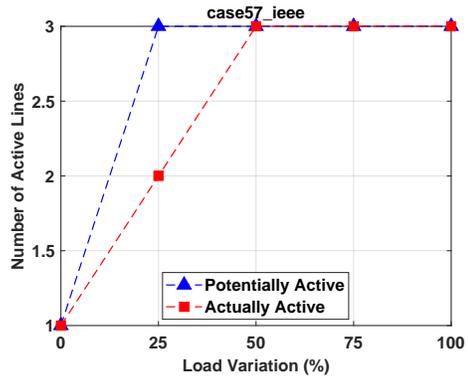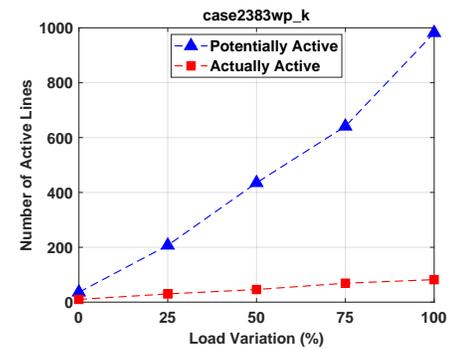

Fig. 3: Number of active lines at each load variation range for (a) case39_epri, (b) case57_ieee, (c) case118_ieee, and (d) case2383wp_k.

buses, as depicted by Fig. 3c (118-bus system) and Fig. 3d (2383-bus system). However, the trend is less apparent in cases with fewer buses, such as case39 (Fig. 3a) and case57 (Fig. 3b), where the gap between the potentially and actually active line flow limits is small regardless of the load variation range. For large systems, this can be explained by noticing that the constraint screening method may identify potentially active line flow limits that are associated with very impractical generator outputs (i.e., choices of generator outputs that are feasible with respect to the DC OPF constraints but very suboptimal in terms of their cost). In comparison, the feasible spaces associated with small systems may not admit the same extremity of impractical generation outputs.

In addition to sampling from a range of load variation as described above, we also considered the number of potentially and actually observed active flow constraints at a set of specific loading conditions, i.e., nominal and heavily loaded (every bus at its maximum load). The heavily loaded condition resulted in more line limits being active compared to the nominal loading. However, both the constraint screening method and the sampling approach found potentially active and observed active line flow limits, respectively, that were not active in either the heavily loaded or the nominal cases.

Overall, the observations show that the number of actually active line flow constraints may be much less than the number identified by constraint screening methods, especially in large systems where the screening methods are most useful. For example, for case2383wp_k with $\pm 100\%$ load variation, the screening method identified 982 potentially active line flow constraints, whereas only 82 active line flow limits were observed in the actual DC OPF results. Even though the screening method has successfully eliminated 1914 redundant line constraints for this system, there remain 900 line flow limits that appear to be inactive for typical objective functions. These results thus suggest the potential for further improvements in identifying inactive line flow limits beyond the capabilities of existing optimization-based constraint screening methods.

C. Characteristics of Redundant and Active Line Constraints

To investigate the sets of redundant and active line flow constraints, we categorized the lines in each test case based on the following two criteria:

1) *Frequency of activeness*: If a line is identified by the screening method as having a non-redundant flow constraint in all five load variation scenarios (0%, $\pm 25\%$, $\pm 50\%$, $\pm 75\%$, and $\pm 100\%$ of the nominal load), then we say that it has a "frequency of activeness" of five. Similarly, if a line is screened to be never active (redundant) for all the load ranges, its frequency of activeness is equal to zero. Hence, six frequency bins can be established for all the transmission lines in each test case.

2) *Potentially-active / actually-active / redundant status*: Section IV-B shows that there are a number of lines that are identified as being potentially active by the screening method, but are never observed to be active in the sampled DC OPF results. Therefore, we separate lines into three categories: (i) potentially active, (ii) potentially

and actually active (active in at least one of the sampled DC OPF solutions), and (iii) redundant/inactive.

From Section II, the power flow on the line between buses m and n is directly proportional to the line's susceptance, b_{mn}, and must be within the line flow limit, f_{mn}^{max}. In this work, b_{mn} is defined as

$$b_{mn} = \frac{1}{x_{mn}}, \tag{5}$$

where x_{mn} is the line reactance. Therefore, the line flow is inversely proportional to x_{mn}.

We hypothesize the following relationships between a line's power flow, rated flow limit (f_{mn}^{max}), and reactance (x_{mn}):

1) A smaller rated limit, f_{mn}^{max}, makes it more likely that the line's flow limit is an active constraint. Small values of f_{mn}^{max} shrink the feasible space for the maximum line flow. Hence, lines with relatively small f_{mn}^{max} would have a greater chance of reaching the line flow limit.

2) A smaller reactance, x_{mn}, increases the possibility that the line's flow limit is an active constraint. Small values of x_{mn} increase the power flow in line mn for a given angle difference since the line flow is inversely proportional to x_{mn}. Therefore, lines with relatively small x_{mn} may have larger power flows, reaching their flow limit and thus being identified as active.

3) If both f_{mn}^{max} and x_{mn} for a particular line are small, i.e., $f_{mn}^{max} \times x_{mn}$ is small, then this line has a greater chance of being an active constraint.

4) Conversely, redundant lines tend to have larger values of f_{mn}^{max} or x_{mn} (and hence, larger values of $f_{mn}^{max} \times x_{mn}$) compared to the rest of the lines.

To test this hypothesis, we plot the mean, maximum, and minimum values of f_{mn}^{max}, x_{mn}, and $f_{mn}^{max} \times x_{mn}$ for all the transmission lines in each test case with respect to their frequency of activeness. A selected subset of the results is shown in Figs. 4–8. As explained before, the frequency of activeness is obtained from the constraint screening method where five indicates a line is identified to be active in all five load scenarios and zero indicates that a line is identified to be redundant in all scenarios. The plots include lines that are identified as potentially active and redundant from the constraint screening method as well as those that are actually active from repeated DC OPF solutions. In these plots, the square marker, top whisker, and bottom whisker represent the mean, maximum, and minimum values of the quantities of interest, i.e., f_{mn}^{max}, x_{mn}, and $f_{mn}^{max} \times x_{mn}$, respectively.

We first observe that lines that are actually active in DC OPF results have a frequency of activeness greater than or equal to 2. This means that they have been identified by the screening method in two or more load variation scenarios. This observation is expected since the feasible space of the screening method is larger compared to DC OPF, and some of the screening results can be non-achievable in solutions to DC OPF problems. The potentially active lines that have a low frequency of activeness of 1, i.e., only identified in one loading scenario, may represent rare or extreme conditions identified by the screening method.

Secondly, we see that the results based on the test cases selected in this work corroborate our hypothesis:

- For case24_ieee_rts, Figs. 4a and 4b show that even though both f_{mn}^{max} and x_{mn} do not exhibit significant difference between redundant and active lines, the range of $f_{mn}^{max} \times x_{mn}$, in Fig. 4c, spans higher values for the redundant lines than the rest of the lines.
- In case30_ieee (Fig. 5), all three quantities of f_{mn}^{max}, x_{mn}, and $f_{mn}^{max} \times x_{mn}$ are noticeably larger for the redundant lines than the active lines.
- f_{mn}^{max} is significantly higher in non-active lines than the rest as demonstrated by Fig. 6a for case240_pserc.
- Both f_{mn}^{max} (Fig. 7a) and x_{mn} (Fig. 7b) are larger in redundant lines than the rest for case300_ieee.
- Fig. 8b for case case2383wp_k shows that the range of x_{mn} spans higher values in redundant lines than the rest.

Overall, it can be seen that lines are more likely to be redundant if at least one of the quantities f_{mn}^{max}, x_{mn}, or $f_{mn}^{max} \times x_{mn}$ are significantly larger than the rest of the lines.

Hence, as future work, it may be possible to design a pre-screening method to identify redundant lines based on examining f_{mn}^{max}, x_{mn}, and $f_{mn}^{max} \times x_{mn}$ to reduce the burden of optimizing every branch's power flow in the constraint screening method. However, the following extensions are necessary to have an accurate and robust pre-screening method:

1) Testing the hypothesis regarding f_{mn}^{max}, x_{mn}, and $f_{mn}^{max} \times x_{mn}$ on a broader range of test cases.
2) Quantifying how large, relatively, these indicators need to be for a line to be reliably classified as redundant.
3) Investigating other indicators that can be potentially used in conjunction with the three studied in this work to provide better pre-screening results. As one avenue for future work, the observations in this paper could be combined with machine learning techniques developed for similar constraint screening purposes [14].

D. Active Lines Observed in DC OPF Cases

In addition to the patterns between potentially and actually active lines, several other patterns are noticeable within the actually active lines themselves. In the 10,000 DC OPF solutions for each load variation range, some lines were active more often than other lines. The graphs in Fig. 9 and Fig. 10 represent the observed active line data from the DC OPF simulations, at $\pm 100\%$ load variation, for the IEEE 39-bus and the PEGASE 89-bus systems, respectively.

In these figures, each node represents a *set of line flow limits* that are simultaneously active in some load-cost combination scenario. The size of the node represents the number of scenarios where the active flow constraints consist of that particular set of lines. A larger node size indicates that this particular set of line flow constraints is active in many scenarios. Each edge indicates the number of lines that are common between the two sets of active lines represented by each terminal node. The thickness of an edge corresponds to the number of common lines between the two nodes. The thickest edges, shown in purple, indicate multiple common lines between the sets of active lines on either end node. The centers of these
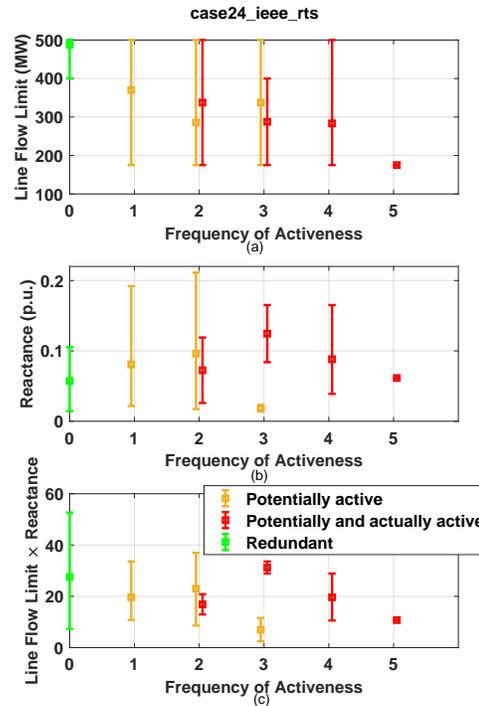

Fig. 4: Line characteristics for case24_ieee_rts: (a) line flow limit, (b) reactance, and (c) line flow limit multiplied by reactance.
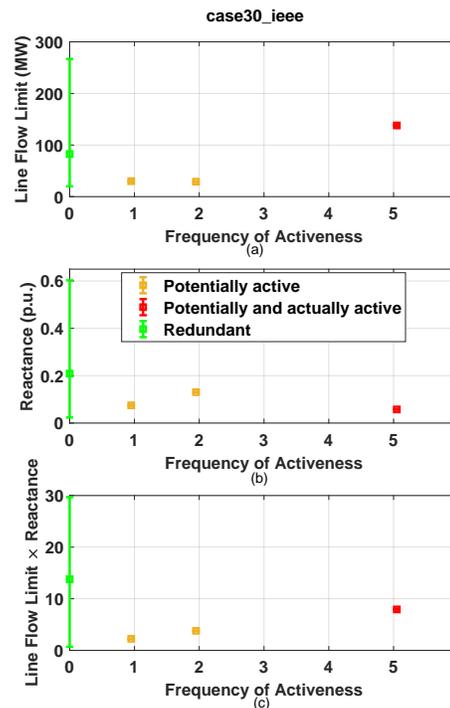

Fig. 5: Line characteristics for case30_ieee: (a) line flow limit, (b) reactance, and (c) line flow limit multiplied by reactance.

Fig. 6: Line characteristics for case240_pserc: (a) line flow limit, (b) reactance, and (c) line flow limit multiplied by reactance.

Fig. 7: Line characteristics for case300_ieee: (a) line flow limit, (b) reactance, and (c) line flow limit multiplied by reactance.
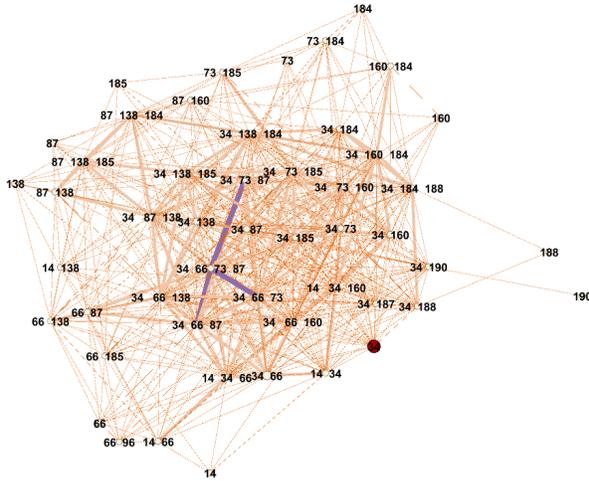

Fig. 8: Line characteristics for case2383wp_k: (a) line flow limit, (b) reactance, and (c) line flow limit multiplied by reactance.

Fig. 9: Case39_epri: sets of actually active lines for every load-cost scenario within the $\pm 100\%$ load variation.

graphs are denser because of the many common active lines. Interestingly, even though DC OPF simulations are conducted over a wide ranges of load variation ($\pm 100\%$) and generator costs, certain sets of line constraints are repeatedly observed to be active. A similar pattern was observed in the constraint screening method as indicated by the frequency of activeness in the previous subsection. These results mean that certain sets of active line flow limits are "more active" than others in most operating conditions. Analyzing which sets of lines lie in the center of these graphs can help operators to narrow down the active constraints to an even smaller subset for most

Fig. 10: Case89_pegase: sets of actually active lines for every load-cost scenario within the ±100% load variation.

operating conditions. Moreover, future extensions which apply graph theoretic tools to analyze the diagrams in Figs. 9–10 hold potential for better understanding relationships among different operational behaviors of power grids.

V. CONCLUSIONS

This paper has investigated both redundant and active line flow constraints in DC OPF problems under a range of load demand and cost function variations. By applying a constraint screening method to identify potentially active line constraints and observing which lines actually reach their flow limits in DC OPF solutions, we have observed that a significant number of line constraints are redundant in all load variation scenarios. Moreover, the number of actually active line constraints is much smaller than the number of potentially active lines in typical large-scale systems. This suggests the potential for further improvements in identifying active line flow constraints beyond the capabilities of existing constraint screening methods.

In addition, we observe the following: (i) lines with redundant constraints typically have larger flow limits and/or line reactances compared to active lines, and (ii) certain sets of line constraints are repeatedly observed to be active even over a large range of load and cost variations. These findings suggest that it may be possible to eliminate redundant line constraints by examining the physical characteristics of each line as a pre-screening step. This can potentially improve the speed of constraint screening methods since such a fast pre-screening step would reduce the number of optimization problems that are solved in the actual screening step.

Future work includes extending the analyses in this paper to consider the impacts of security constraints [15] as well as modifying constraint screening methods to achieve the potential benefits suggested by our results. Inspired by the success of *optimality-based* bound tightening techniques that have been applied to relaxations of AC optimal power flow problems [16], [17], one avenue for improving constraint

screening methods is to incorporate information from the cost function into constraint screening methods.

REFERENCES

[1] S. Lumbreras and A. Ramos, "The new challenges to transmission expansion planning. Survey of recent practice and literature review," *Electric Power Systems Research*, vol. 134, pp. 19–29, 2016.

[2] W. van Ackooij, I. Danti Lopez, A. Frangioni, F. Lacalandra, and M. Tahanan, "Large-scale unit commitment under uncertainty: An updated literature survey," *Annals of Operations Research*, vol. 271, no. 1, pp. 11–85, December 2018.

[3] A. J. Ardakani and F. Bouffard, "Identification of umbrella constraints in DC-based security-constrained optimal power flow," *IEEE Transactions on Power Systems*, vol. 28, no. 4, pp. 3924–3934, Nov 2013.

[4] ——, "Acceleration of umbrella constraint discovery in generation scheduling problems," *IEEE Transactions on Power Systems*, vol. 30, no. 4, pp. 2100–2109, July 2015.

[5] R. Madani, J. Lavaei, and R. Baldick, "Constraint screening for security analysis of power networks," *IEEE Transactions on Power Systems*, vol. 32, no. 3, pp. 1828–1838, May 2017.

[6] L. A. Roald and D. K. Molzahn, "Implied constraint satisfaction in power system optimization: The impacts of load variations," in *57th Annual Allerton Conference on Communication, Control, and Computing*, September 2019.

[7] A. S. Xavier, F. Qiu, F. Wang, and P. R. Thimmapuram, "Transmission constraint filtering in large-scale security-constrained unit commitment," *IEEE Transactions on Power Systems*, vol. 34, no. 3, pp. 2457–2460, May 2019.

[8] Y. Ng, S. Misra, L. A. Roald, and S. Backhaus, "Statistical learning for DC optimal power flow," in *20th Power Systems Computation Conference (PSCC)*, June 2018, pp. 1–7.

[9] D. K. Molzahn, "Identifying redundant flow limits on parallel lines," *IEEE Transactions on Power Systems*, vol. 33, no. 3, pp. 3210–3212, May 2018.

[10] B. Stott, J. Jardim, and O. Alsaç, "DC power flow revisited," *IEEE Transactions on Power Systems*, vol. 24, no. 3, pp. 1290–1300, August 2009.

[11] M. Grant and S. Boyd, "CVX: Matlab software for disciplined convex programming, version 2.1," http://cvxr.com/cvx, Mar. 2014.

[12] R. D. Zimmerman, C. E. Murillo-Sánchez, and R. J. Thomas, "MATPOWER: Steady-state operations, planning, and analysis tools for power systems research and education," *IEEE Transactions on Power Systems*, vol. 26, no. 1, pp. 12–19, Feb 2011.

[13] S. Babaeinejadsarookolaee, A. Birchfield, R. D. Christie, C. Coffrin, C. L. DeMarco, R. Diao, M. Ferris, S. Fliscounakis, S. Greene, R. Huang, C. Josz, R. Korab, B. C. Lesieutre, J. Maeght, D. Molzahn, T. J. Overbye, P. Panciatici, B. Park, J. Snodgrass, and R. D. Zimmerman, "The power grid library for benchmarking AC optimal power flow algorithms," *arXiv:1908.02788*, 2019.

[14] A. Jahanbani Ardakani and F. Bouffard, "Prediction of umbrella constraints," in *20th Power Systems Computation Conference (PSCC)*, June 2018.

[15] B. Stott, O. Alsaç, and A. J. Monticelli, "Security analysis and optimization," *Proceedings of the IEEE*, vol. 75, no. 12, pp. 1623–1644, December 1987.

[16] M. Lu, H. Nagarajan, R. Bent, S. D. Eksioglu, and S. J. Mason, "Tight piecewise convex relaxations for global optimization of optimal power flow," in *20th Power Systems Computation Conference (PSCC)*, June 2018.

[17] M. Bynum, A. Castillo, J.-P. Watson, and C. Laird, "Tightening McCormick relaxations toward global solution of the ACOPF problem," *IEEE Transactions on Power Systems*, vol. 34, no. 1, pp. 814–817, January 2019.